

Steady-State Luminescence of Polymers: Effects of Flow and of Hydrodynamic Interactions

Ramon Reigada

Facultat de Química, Universitat de Barcelona,
C/ Martí i Franquès 1, 08028 Barcelona, Spain
e-mail: reigada@ub.edu

Igor M. Sokolov

Institut für Physik, Humboldt-Universität zu Berlin,
Newtonstr. 15, D-12489 Berlin, Germany
e-mail: igor.sokolov@physik.hu-berlin.de

November 19, 2018

Abstract

We consider a simple model for steady-state luminescence of single polymer chains in a dilute solution in the case when excitation quenching is due to energy transfer between a donor and an acceptor attached to the ends of the chain. We present numerical results for Rouse chains without or with hydrodynamic interactions, which are taken into account in a perturbative manner. We consider the situations of a quiescent solvent as well as the chain in a shear flow and discuss the dependence of the steady-state luminescence intensity on the strength of hydrodynamic interaction and on the shear rate in the flow.

1 Introduction

Luminescent energy transfer in polymers is an important phenomenon. Luminescent markers are used both for probing the intrinsic polymer dynamics, and for probing the properties of the environment using polymers. However, the theory of such dynamical phenomena is to no extent satisfactory. The problem here is the complicated nonmarkovian dynamics of the system, where the most interesting phenomena take place on the time-scales on which the systems shows strong memory effects. Even the corresponding initial condition problem is hard to solve. No satisfactory quantitative theory exists at present for the stationary case.

Let us start from formulating the problem, and discuss the simplest energy transfer model, which will be used throughout the article. Let us assume that the ends of a polymer are marked by a donor and an acceptor monomers. The molecule is under constant irradiation at a resonant probe frequency, so that the donor can get excited with probability λ per unit time (we consider λ as effective intensity of the irradiation). The relaxation of the excited state due to spontaneous emission, as well as nonlinear effects connected with possible multiple excitation are neglected, so that the only mechanism of relaxation is the donor-acceptor energy transfer. We assume that the corresponding energy transfer is accompanied by emission of a photon with the frequency different from one of the irradiating light. This transfer takes place when donor and acceptor approach each other at distance a , hereafter called reaction radius. Physically, two situations may take place: Being in vicinity of the acceptor the donor still can be excited, and immediately emits a photon at the observation frequency. Another situation is the one when, being close to the acceptor, the donor gets out of resonance with the probe and cannot be excited. In this case, the donor-acceptor system may be in one of the two states, *on* and *off*; being in the *on*-state the system may be excited with probability λ per unit time, and emits the photon under the transition into the *off*-state. In what follows the expressions *on* and *off* will be simply used for denoting states in which the end-to-end distance is above and below the reaction radius a , respectively.

The overall situation might seem simple, however it is much more complicated than the case of irreversible cyclization [1–7] and is extremely awkward for theoretical investigation, even in the absence of flow. Our knowledge about the reaction kinetics under flow is sporadic even for simpler reactions, see [8, 9].

The whole problem would be easily solvable if the life time distributions in the *on*- and the *off*-states were known. Then the probability to be excited being in the *on*-state and therefore the intensity of the emitted light could be easily calculated. The probabilities to be in the either state are connected with the level-crossing properties of the random process $r(t)$, where $r(t)$ is the instantaneous end-to-end distance of the polymer. As for all diffusive processes, however, the level-crossing process by $r(t)$ shows a fractal structure, so that the mean time between two such crossings is zero (this follows immediately from the Rice formula for level crossing density and from the form of the two-time correlation function of the end-to-end distances, say, for a Rouse polymer, which function lacks the second derivative at zero). Again, as for all diffusive processes, this leads to a "tremor" in which $r(t)$ crosses the a -level many times until it leaves and performs a long excursion to either side. This "tremor" is due to the fact that the diffusion approximation (Wiener process) used in the description of the chain (for example through the Rouse-like Langevin dynamics) does not adequately mirror a short-time dynamics of whatever physical system [10]. However, the existence of this theoretical problem does to no extent require for the change of the model (say, by introducing underdamped dynamics, as proposed in [10]) since the physical problem at hand does not depend on the too-small time behavior of the $r(t)$ -process. Indeed, this process is randomly sampled at times t_i given by a Poissonian flow of photons following with the rate λ . The behavior of $r(t)$ at times much smaller than λ^{-1} thus cannot be sampled and can physically play no role: this statement is a close analogue of the Nyquist's sampling theorem. Thus, the absence of the life-time distributions is not a problem of our theoretical model, but a problem of standard mathematical tools which rely too much on unphysical, but absolutely unimportant short-time properties of a Wiener process.

Therefore in what follows we concentrate on the numerical investigation of the proposed model, and consider the intensity of stationary luminescence of the polymer $I(\lambda)$ under constant irradiation. We discuss the Rouse model without hydrodynamic interactions, as well as the role of hydrodynamic interaction between the monomers, and consider the case when the polymer molecule undergoes deformation in a (weak enough) shear flow, which does not however cause the full stretching of the molecule. This situation is especially interesting as the case when the stationary luminescence of diluted polymer solution can be used as a probe for the flow structure. Authors are not aware of any experimental realizations of such visualization method, thus

our theoretical study might serve as a proof-of-principle for such immediate flow diagnostics method.

2 Simulation approach

Let us start from discussing our numerical algorithm. Our simulations consist of two independent parts: the simulation of the $r(t)$ -trajectories, which are then stored with high enough resolution, and their analysis giving the steady-state luminescence intensity. The reason for this approach is that one realization of the process can then be used for getting $I(\lambda)$ for a variety of parameters a and λ of the model, so that the most time-consuming part of the simulation has to be done only once for exactly the time necessary to get enough statistics.

Let us concentrate first of the last part of the problem, namely on the evaluation of the stationary luminescence intensity for a given realization of $r(t)$ -process. From the record of the $r(t)$ (time resolution of stored data has to be much smaller than the minimal λ^{-1} used in simulations) we define the a -crossings of the process and, for given a , obtain the lengths of *on*- and *off*-intervals, which are ordered and stored. According to the Poisson statistics, the probability not to get excited during the *on*-interval of duration t_{on} is exactly $\exp(-\lambda t_{on})$, thus the probability to emit light after the *on*-excursion is equal to $1 - \exp(-\lambda t_{on})$. Since the intensity of emitted light is proportional to the overall number of the intervals during which the system made a transition into its excited state, we have for the model where the *off*-state is not excitable:

$$I(\lambda) = \frac{1}{T} \sum_{i=1}^{n(a,T)} [1 - \exp(-\lambda t_i)] \quad (1)$$

where i numbers the *on*-intervals, $n(a,T)$ is their overall number, which depends on the reaction radius a and on the overall time of simulations T . Equation (1) shows that the intervals of very small duration are sampled with the probability proportional to their lengths so that, as anticipated, the fractal structures in vicinity of the concentration points of the level-crossings are not resolved and play no role. Using Eq.(1) it is possible to scan the whole range of intensities λ within one run, which is necessary to detect nonlinear effects. The situation in which, being in the *off*-state, the

molecule immediately emits light, can be taken into account by adding the corresponding intensity to the expression given by Eq.(1),

$$I_1(\lambda) = I(\lambda) + \lambda P_{off} \quad (2)$$

where P_{off} is the probability to be in the *off*-state, i.e. the overall relative time spent below a . For example, for the case without flow, it is simply a function of relative reaction radius $\rho = a/\sqrt{\langle L^2 \rangle}$, where $\langle L^2 \rangle$ is the mean end-to-end squared distance for the chain,

$$P_{off}(\rho) = \text{erf}\left(\sqrt{\frac{3}{2}}\rho\right) - \rho\sqrt{\frac{6}{\pi}}\exp\left(-\frac{3}{2}\rho^2\right). \quad (3)$$

Since this simply corresponds to adding a linear function of λ to the results for the *on-off* model, we concentrate in what follows only on these results, given by Eq.(1). This result holds for all situations without flow. In the situation with flow and with hydrodynamic interactions, it is hard to get the analytical expression for P_{off} . The numerical results following from our simulations are presented in Tables 3 and 4.

Let us now turn to simulation of the trajectories.

2.1 The Rouse model

We start from the Rouse chain as the simplest model for a polymer [11, 12]. A Rouse chain is a set of N beads; each one, except for the two end beads, is connected to two neighbors by a harmonic potential, so that the overall potential energy of the system reads

$$V = \sum_{i=1}^{N-1} \frac{1}{2} k |\vec{r}_i - \vec{r}_{i+1}|^2, \quad (4)$$

where k is the harmonic spring constant and \vec{r}_i corresponds to the position of the i -th bead. The end beads are connected only to one neighbor. The equation of motion of the chain corresponds to overdamped motion under the influence of thermal fluctuations:

$$\dot{\vec{r}}_i = -\frac{1}{\gamma} \frac{\partial V}{\partial \vec{r}_i} + \frac{1}{\gamma} \vec{\eta}_i, \quad (5)$$

where γ is the friction parameter and $\vec{\eta}_i$ is a zero-mean white noise obeying the fluctuation-dissipation relation,

$$\langle \eta_i^\alpha(t) \eta_j^\beta(t') \rangle = 2k_B T \gamma \delta_{ij} \delta_{\alpha\beta} \delta(t - t'). \quad (6)$$

In thermal equilibrium, the following relations following immediately from the canonical distribution have to hold independently on the model (and are always checked numerically as a proof of the quality of the simulation):

$$\langle E_{tot} \rangle = \frac{3}{2}(N - 1)k_B T \quad (7)$$

$$\langle d^2 \rangle = \sqrt{\frac{3k_B T}{k}} \quad (8)$$

$$\langle L^2 \rangle = \frac{3(N - 1)k_B T}{k}, \quad (9)$$

where E_{tot} is the total energy, and d and L stand for the bead-to-bead and end-to-end distances, respectively.

We also now apply a shear flow to the system, $\vec{v} = (\alpha y, 0, 0)$. The shear flow is implemented in Eqs.(5) by including a term $+\alpha y_i$ for the motion in the x -coordinate of each bead i ,

$$\dot{\vec{r}}_i = -\frac{1}{\gamma} \frac{\partial V}{\partial \vec{r}_i} + \frac{1}{\gamma} \vec{\eta}_i + (\alpha y_i, 0, 0). \quad (10)$$

The characteristic intensity of the flow necessary to compare its effects on the chain's conformation in different situations is given by the value of the dimensionless parameter $\alpha \tau_R$ with τ_R being the Rouse time [7].

2.2 Hydrodynamic interactions

The situation under hydrodynamic interactions is much more involved. The standard approaches [13–15] are very accurate but slow, so that we prefer an approximate perturbative one. The quality of the corresponding approximations is checked by calculating two thermodynamically fixed parameters of the chain in quiescent solvent: its mean end-to-end distance and the overall energy. We anticipate that especially the end-to-end distance in the chain was found to be extremely sensitive to improper incorporation of the hydrodynamic interaction. We confined ourselves to the situations under which the first order of the perturbation theory was found sufficient.

The hydrodynamic interactions among the beads are modeled within the Zimm scheme [16]. The Zimm model is based on the Rouse chain model but the equations of motion for different beads are coupled to each other not only through elastic forces but also through hydrodynamic forces. Such coupling is a long-range one and is introduced through the Oseen tensor [17], that is a 3×3 tensor defined for each pair of beads (i - j),

$$\mathcal{H}_{ij} = \frac{1}{8\pi\eta|\vec{r}_{ij}|} \left[\vec{r}'_{ij} (\vec{r}'_{ij})^T + \mathcal{I} \right] \quad (11)$$

$$\mathcal{H}_{ii} = \frac{1}{\gamma} \mathcal{I}, \quad (12)$$

where \mathcal{I} is a unit matrix, \vec{r}'_{ij} is a unit vector $\vec{r}_{ij}/|\vec{r}_{ij}|$ in the direction of \vec{r}_{ij} and $(\vec{r}'_{ij})^T$ is its transpose. The viscosity parameter η can be expressed through γ and the bead's size r_0 since for $i = j$ one has $1/6\pi\eta r_0 = 1/\gamma$. Then,

$$\mathcal{H}_{ij} = \frac{3r_0}{4\gamma|\vec{r}_{ij}|} \left[\vec{r}'_{ij} (\vec{r}'_{ij})^T + \mathcal{I} \right]. \quad (13)$$

In what follows we use $\gamma = 1$. The equation of motion for the i -th bead thus reads:

$$\dot{\vec{r}}_i = \sum_{j=1}^N \mathcal{H}_{ij} \left(\frac{\partial V}{\partial \vec{r}_j} + \vec{\eta}_j \right). \quad (14)$$

The noises $\vec{\eta}_j$ acting on different beads are now not independent, otherwise the fluctuation-dissipation theorem would be violated. One often writes the corresponding equation of motion in the form

$$\dot{\vec{r}}_i = \mathcal{H} \vec{f}_i + 2k_B T \mathcal{A} \vec{\psi}, \quad (15)$$

where \mathcal{H} is the $3N \times 3N$ matrix with the diagonal elements being unity (in the units where $\gamma = 1$) and with the nondiagonal elements denoting the Oseen terms between the corresponding components of velocity of different beads, and the matrix $\mathcal{A} = \sqrt{\mathcal{H}}$ is defined through $\mathcal{A} \cdot \mathcal{A}^T = \mathcal{H}$. The elements of the vector $\vec{\psi}$ are now independent, zero mean Gaussian white noises. Actually,

the computation of the equations of motions in the Euler scheme reads,

$$\begin{pmatrix} x_1(t + \Delta t) \\ y_1(t + \Delta t) \\ z_1(t + \Delta t) \\ x_2(t + \Delta t) \\ \dots \\ \dots \\ \dots \end{pmatrix} = \begin{pmatrix} x_1(t) \\ y_1(t) \\ z_1(t) \\ x_2(t) \\ \dots \\ \dots \\ \dots \end{pmatrix} + \Delta t \mathcal{H} \begin{pmatrix} f_1^x(t) \\ f_1^y(t) \\ f_1^z(t) \\ f_2^x(t) \\ \dots \\ \dots \\ \dots \end{pmatrix} + \sqrt{2k_B T \Delta t} \mathcal{A} \begin{pmatrix} \psi_1^x(t) \\ \psi_1^y(t) \\ \psi_1^z(t) \\ \psi_2^x(t) \\ \dots \\ \dots \\ \dots \end{pmatrix}, \quad (16)$$

where f_i^β are the forces due to the harmonic springs for the i -th bead in the β axis and ψ_i^β are the corresponding components of $\vec{\psi}$.

The computation of \mathcal{A} can be performed exactly by diagonalizing \mathcal{H} . This exact diagonalization requires an extremely high computational cost for long chains. The widely used method based on the orthogonal polynomials decomposition (which gives very exact results) is still too slow to get the runs long enough for our purposes. Therefore we decided for a simple approximate approach based on the perturbation expansion of the hydrodynamic interaction.

To do this we write \mathcal{H} as $\mathcal{I} + r_0 \mathcal{S}$, and then expand the square root $\mathcal{A} = \sqrt{\mathcal{I} + r_0 \mathcal{S}}$ in powers of r_0 ,

$$\mathcal{A} \approx \mathcal{I} + \frac{r_0 \mathcal{S}}{2} - \frac{r_0^2 \mathcal{S}^2}{8} + \dots \quad (17)$$

Since in the thermal equilibrium the averages $\langle E_{tot} \rangle$ being the internal energy and $\langle L^2 \rangle$ (also being a thermodynamical quantity following immediately from equipartition) are not modified by the dissipative coupling introduced by the Oseen tensor, we can numerically check the validity of the approximations for \mathcal{A} for different r_0 values. We see that $\langle L^2 \rangle$ is extremely sensitive to incorrect incorporation of the hydrodynamic interaction, and its calculation is used as a probe of the quality of the approximation, see Tables 1 and 2. The data for Rouse model give us typical error bars for the simulation of the exact model on the same scale.

Looking at the Tables 1 and 2, one can conclude that for r_0 up to 0.2, the second order approximation is sufficient, and for r_0 up to 0.1, the first order approximation (much shorter simulations) is accurate enough. In the case $r_0 = 0.5$ also the second order gets insufficient. Thus, in our simulations we restrict ourselves to $r_0 \leq 0.2$. We use a second order Runge-Kutta

Table 1: The quality of perturbative approximations for $N = 21$

		$\langle E_{tot} \rangle$	$\langle L^2 \rangle$
Theoretical		30	20
Rouse simulation		30.185	21.028
Zimm, $r_0 = 0.1$	0-order	29.591	27.406
	1-order	30.763	21.020
	2-order	30.221	20.181
Zimm, $r_0 = 0.2$	0-order	31.190	36.923
	1-order	33.114	23.843
	2-order	31.676	21.839
Zimm, $r_0 = 0.5$	0-order	42.058	73.349
	1-order	49.344	44.741
	2-order	53.215	46.732

method to solve Eqs.(16) with a sufficiently small time step $\Delta t = 10^{-3}$. For the results shown in this paper we run $2 \cdot 10^7$ iterations up to a maximum time $t = 2 \cdot 10^4$ for a full trajectory needed for adequate statistics. An initial thermalization period of 1000 time units is performed in all cases in order to start the trajectories from a thermal equilibrium state. The *Compaq AlphaServer HPC320* used to run these simulations requires about 3 hours of CPU time for $N = 51$ when the first order approximation scheme is chosen. The second perturbative order requires more than 120 hours of CPU time for the same number of iterations and chain length.

3 Results

Although the overall role of flow and hydrodynamical interaction is rather clear, the behavior of the intensity as a function of parameters α and r_0 is not trivial. The flow elongates the molecule, so that the typical end-to-end distance grows with α while the hydrodynamical interactions slow-down the dynamics of intramolecular relative motion, which increases the characteristic time spent in *on*-state.

The behavior of $I(\lambda)$ as a function of hydrodynamic radius and flow intensity strongly depends on the relation ρ between the reaction radius, a , and the equilibrium end-to-end distance of the polymer (i.e. the one in the

Table 2: The quality of perturbative approximations for $N = 51$

$N = 51$		$\langle E_{tot} \rangle$	$\langle L^2 \rangle$
Theoretical		75	50
Rouse simulation		75.323	48.122
Zimm, $r_0 = 0.1$	0-order	76.063	86.674
	1-order	77.412	54.021
	2-order	75.926	47.746
Zimm, $r_0 = 0.2$	0-order	81.399	130.64
	1-order	83.903	67.487
	2-order	79.167	51.600

absence of the flow), $L = \sqrt{\langle L^2 \rangle}$. For $\rho \ll 1$ the polymer is typically in the *on*-state, and thus the flow (elongating the chain and making the transition into the *off*-state less probable) and the hydrodynamic interaction without flow (making the change of states slower) work in the same direction and lead to the decrease in intensity, as it is clearly seen in Fig.1.

For $\rho \gg 1$ the molecule is typically in the *off*-state. Increasing flow increases the probability of switching to the *on*-state, and thus leads to increase in the steady-state intensity. The hydrodynamic interaction in the absence of the flow also leads to increasing the typical time in the corresponding state. The effects of the flow and the hydrodynamic interactions for $\rho \gg 1$ are depicted in Fig.2. The increasing effect of the hydrodynamic interaction has to do with the interplay of two factors. On the one hand, the longer *on*-intervals get even longer under hydrodynamic interaction, and thus give smaller contributions to the overall intensity. On the other hand, increasing the interaction makes that more shorter *on*-intervals are now resolved on the timescale of λ^{-1} , and these contributions in the intensity overweigh the loss due to the former of both effects.

This explanation shows that the role of hydrodynamic interaction is rather subtle, and may lead to interesting effects for both regimes ($\rho \ll 1$ and $\rho \gg 1$), especially when the flow is present. Indeed, the effect of hydrodynamic interaction for the cases with $\alpha \neq 0$ depends in a fine way on all parameters, and may act in opposite directions (compare the curves for no flow and high flow, $\alpha\tau_R = 6.56$, in both panels of Fig.1, and the curves for no flow and moderate flow, $\alpha\tau_R = 1.05$, in the upper panel of Fig.2).

The values of P_{off} which are necessary to establish the connection be-

tween the two situations discussed in the Introduction (Eq.(2)) are given in Tables 3 and 4 for $N = 21$ and for $N = 51$, respectively. The intensities of the flows in these tables correspond to the same values of the dimensionless flow intensities $\alpha\tau_R = 0, 0.176, 1.05$ and 6.56 for $N = 21$ and for $N = 51$ chains (the Rouse times being $\tau_R = 13.51$ and $\tau_R = 84.43$, respectively).

4 Conclusions

We presented the results of numerical simulations of the intensity of steady-state luminescence of single polymer chains in a dilute solution due to excitation quenching in a simple model in which donor and acceptor are attached to the ends of the chain. The chain is modeled by simple Rouse dynamics without or with hydrodynamic interactions, which are taken into account in a perturbative manner. We consider the situations of a quiescent solvent as well as the chain in a shear flow. Depending on the relation between the effective distance for energy transfer and the typical end-to-end distance of the chain different regimes are encountered with respect to dependence of the steady-state luminescence intensity on the strengths of the flow and of interaction. Such luminescent probes may be used for experimental flow diagnostics.

5 Acknowledgments

The authors acknowledge helpful discussions with J.M. Sancho and F. Sagues. We thank CESCO (Centre de Supercomputació de Catalunya) for financial and computational support through the 'Improving the Human Potential' Program. IMS gratefully acknowledges partial financial support by the Fonds der Chemischen Industrie.

Table 3: P_{off} for the chain with $N = 21$

$\alpha = 0$	$a = 1$	$a = 4$	$a = 8$
$r_0 = 0$	0.014843	0.502626	0.974239
$r_0 = 0.05$	0.014831	0.499207	0.972863
$r_0 = 0.1$	0.013845	0.484438	0.969214
$\alpha = 0.0125$	$a = 1$	$a = 4$	$a = 8$
$r_0 = 0$	0.01467	0.49977	0.97302
$r_0 = 0.05$	0.01481	0.49775	0.97191
$r_0 = 0.1$	0.013724	0.48283	0.96835
$\alpha = 0.078$	$a = 1$	$a = 4$	$a = 8$
$r_0 = 0$	0.013605	0.443851	0.937554
$r_0 = 0.05$	0.013742	0.456638	0.947050
$r_0 = 0.1$	0.012997	0.450992	0.949065
$\alpha = 0.488$	$a = 1$	$a = 4$	$a = 8$
$r_0 = 0$	0.006830	0.15618	0.43874
$r_0 = 0.05$	0.007423	0.18520	0.52606
$r_0 = 0.1$	0.008600	0.20918	0.58951

Table 4: P_{off} for the chain with $N = 51$

$\alpha = 0$	$a = 2$	$a = 7$	$a = 12$
$r_0 = 0$	0.034207	0.613049	0.960062
$r_0 = 0.05$	0.033190	0.594208	0.957482
$r_0 = 0.1$	0.028929	0.556314	0.945990
$\alpha = 0.002$	$a = 2$	$a = 7$	$a = 12$
$r_0 = 0$	0.03386	0.61418	0.95983
$r_0 = 0.05$	0.03270	0.59412	0.95756
$r_0 = 0.1$	0.02932	0.55641	0.94633
$\alpha = 0.0125$	$a = 2$	$a = 7$	$a = 12$
$r_0 = 0$	0.033417	0.575235	0.933795
$r_0 = 0.05$	0.030730	0.571878	0.945019
$r_0 = 0.1$	0.027587	0.540211	0.939310
$\alpha = 0.078$	$a = 2$	$a = 7$	$a = 12$
$r_0 = 0$	0.01609	0.20126	0.45965
$r_0 = 0.05$	0.02417	0.28267	0.61573
$r_0 = 0.1$	0.01273	0.30860	0.67650

References

- [1] G. Wilemski and M. Fixman, J. Chem. Phys. **60**, 866 (1974); *ibid.* 878 (1974)
- [2] M. Doi, Chem. Phys. **9**, 455 (1975)
- [3] A. Szabo, K. Schulten, and Z. Schulten, J. Chem. Phys. **74**, 4350 (1980)
- [4] P.G. de Gennes, J. Chem. Phys. **76**, 3316 (1982)
- [5] R.W. Pastor, R. Zwanzig, and A. Szabo, J. Chem. Phys. **105**, 3878 (1996)
- [6] T. Bandyopadhyay and S.K. Ghosh, J. Chem. Phys. **116**, 4366 (2002)
- [7] I.M. Sokolov, Phys. Rev. Lett. **90** 080601 (2003)
- [8] G.H. Fredrickson and L. Leibler, Macromolecules, **29** 2674 (1996)
- [9] A. Kolb, C.M. Marques and G.H. Fredrickson, Macromol. Theory and Simul., **6**, 169 (1997)
- [10] R.S. Eisenberg, M.M. Klosek and Z. Schuss, J. Chem. Phys. **102** 1767 (1995)
- [11] P.E. Rouse, J. Chem. Phys. **21**, 1272 (1953)
- [12] F. Bueche, J. Chem. Phys. **22**, 603 (1954)
- [13] M. Fixman, Macromolecules **19**, 1204 (1986)
- [14] R. Rzehak, D. Kienle, T. Kawakatsu and W. Zimmermann, Europhys. Lett. **46**, 821 (1999)
- [15] R. Rzehak and W. Zimmermann, Europhys. Lett. **59**, 779 (2002)
- [16] B.H. Zimm, J. Chem. Phys. **24**, 269 (1956)
- [17] M. Doi and S.F. Edwards, *The Theory of Polymer Dynamics*, Cornell University Press, Ithaca, NY (1981)

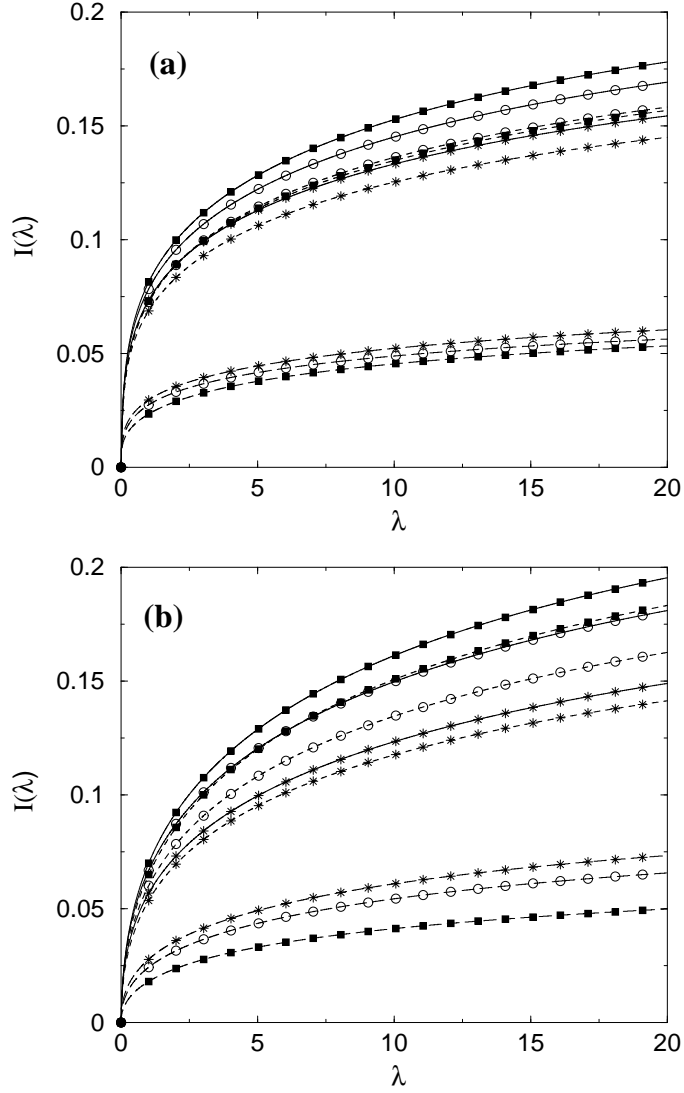


Figure 1: The intensity of steady-state luminescence in the *on-off* model as a function of irradiation intensity λ for a reaction radius such that $\rho \ll 1$. In panel (a) $N = 21$ and $a = 1$. In panel (b) $N = 51$ and $a = 2$. In both panels the same notation is used: the symbol indicates the value of the bead radius r_0 : filled squares (0), empty circles (0.05) and stars (0.1), whereas solid, dotted and dashed lines correspond to $\alpha\tau_R = 0$, 1.05 and 6.56, respectively. $\tau_R = 13.51$ for the chain with 21 beads and $\tau_R = 84.43$ for chains with 51 beads.

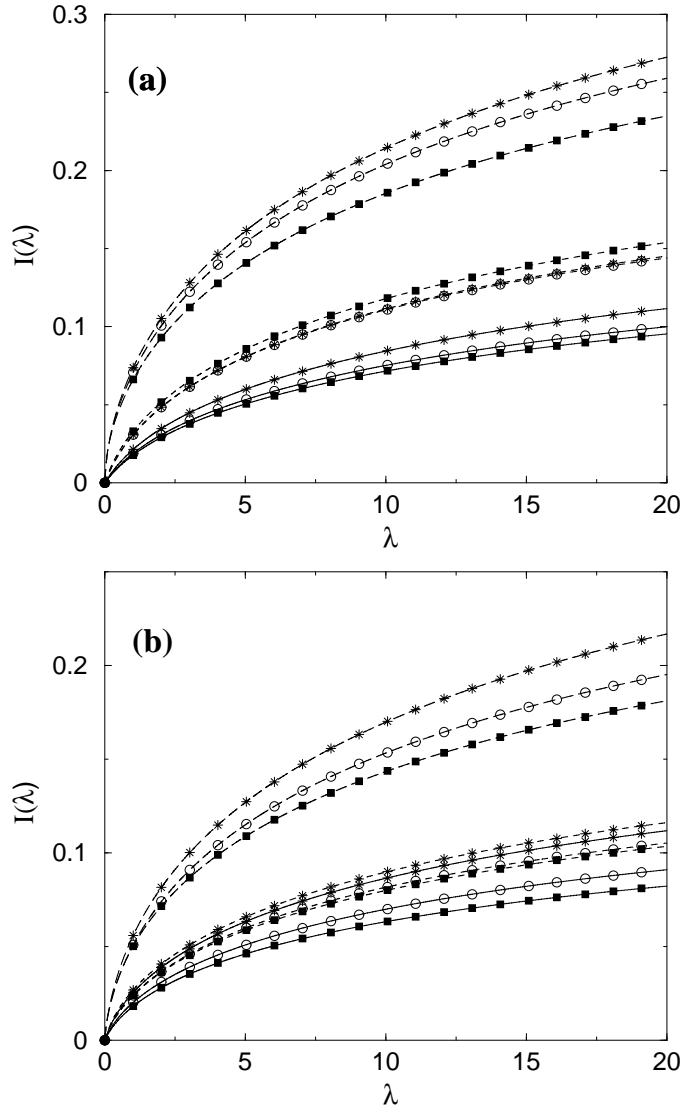


Figure 2: Same as in Fig.1, but now for $\rho \gg 1$. In panel (a) $N = 21$ and $a = 8$. In panel (b) $N = 51$ and $a = 12$. We use the same notation for the lines as in Fig.1